A microfluidic platform for probing single cell plasma membranes using optically trapped Smart Droplet Microtools (SDMs)

Peter M. P. Lanigan,[a] Tanja Ninkovic,[a] Karen Chan,[a] Andrew J. de Mello,[ac] Keith R. Willison,[ad] David R. Klug,[ac] Richard H. Templer,[ac] Mark A. A. Neil*[ab] and Oscar Ces*[ac]

Received 26th September 2008, Accepted 12th December 2008
First published as an Advance Article on the web 21st January 2009
DOI: 10.1039/b816857a

We recently introduced a novel platform based upon optically trapped lipid coated oil droplets (Smart Droplet Microtools—SDMs) that were able to form membrane tethers upon fusion with the plasma membrane of single cells. Material transfer from the plasma membrane to the droplet *via* the tether was seen to occur. Here we present a customised version of the SDM approach based upon detergent coated droplets deployed within a microfluidic format. These droplets are able to differentially solubilise the plasma membrane of single cells with spatial selectivity and without forming membrane tethers. The microfluidic format facilitates separation of the target cells from the bulk SDM population and from downstream analysis modules. Material transfer from the cell to the SDM was monitored by tracking membrane localized EGFP.

1.0 Introduction

In response to the observation of cellular heterogeneity in bacterial and eukaryotic cells[1–4] new technologies are being sought with a view to overcoming the problems associated with the measurement of averages derived from large populations. Despite the wealth of information that current proteomic and genomic platforms are able to provide their reliance on large populations of cells often means that they miss rare events and are difficult to translate to low abundance systems such as progenitor stem cells. The latter can lead to misleading interpretation of biological phenomena.

While genomic sequencing provides critical data pertaining to the building blocks of biological networks, it is limited in providing insights with respect to how the components of a cell come together in both time *and* space in localized cellular processes and subsequent higher order functions. This is a damaging oversight as the complex and spatially dependent nature of signalling pathway networks, the influence of different cellular environments and the phase in the cell cycle and their reliance upon low abundant molecules leads to stochastic behaviour that promotes cellular heterogeneity.[5] The noise in cells is manifest in a variety of processes ranging from the noise-driven divergence of cell fates through to protein expression levels within a single cell and noise-induced amplification of signals.[6] An increased understanding of individual cell responses to therapeutic interventions and the link between biological heterogeneity and signalling pathway control that may underpin given disease states require the use of single cell analysis techniques.[7,8]

1.1 Single cell analysis methods

Recent technological advances have shown that it is possible to measure protein expression levels in single cells using fluorescence based methods.[9,10] We recently introduced a flexible platform technology based upon optically trapped Smart Droplet Microtools (SDMs) that is capable of performing spatially selective upstream examination of membrane proteins from a single cell.[11] The SDMs selected, typically 1–4 microns in size, composed of a hexadecane hydrocarbon core and fusogenic lipid outer coating (a mixture of 1,2-dioleoyl-phosphatidylethanolamine and 1,2-dioleoyl-sn-glycero-3-phosphatidylcholine) were brought into controlled contact with target colon cancer cells leading to the formation of connecting membrane tethers. Material transfer from the cell of interest to the SDM *via* this membrane junction was observed *via* the translocation of membrane localized enhanced green fluorescent protein (EGFP) to the droplet. The upstream separation of the plasma membrane coupled with these fluorescence based technologies could translate to a high-throughput parallel analysis platform in the future.

The approach of selectively analyzing a single cell is not a new one. An increasing number of groups have developed microfluidic modules capable of effecting single cell measurements.[12,13] Current examples for high speed full cell lysis in microfluidic environments include the application of laser pulses,[14,15] electrical fields,[16] mechanical shear forces,[5] chemical treatment[17] and electroporation.[18] Most of these techniques however do not allow sequential measurements to be conducted on a single cell as they result in full cell lysis and thus restrict the ability to unravel the temporal dependence of biological signals. Approaches such as those pioneered by Dragavon[19] are opening up the possibility of probing single cell systems as a function of time without loss of cell viability. They have also shown that it is possible to use

[a]*The Single Cell Proteomics Group, Chemical Biology Centre (CBC), Imperial College London, Exhibition Road, London, UK SW7 2AZ. E-mail: mark.neil@imperial.ac.uk; o.ces@imperial.ac.uk*
[b]*Department of Physics, Imperial College London, Exhibition Road, London, UK SW7 2AZ*
[c]*Department of Chemistry, Imperial College London, Exhibition Road, London, UK SW7 2AZ*
[d]*The Institute of Cancer Research, Chester Beatty Laboratories, 237 Fulham Road, London, UK SW3 6JB*

a cellular isolation system to monitor single cell oxygen consumption rates in real time.

The ability to measure the spatial dependence of biological signals and concentration levels is also critical. Capillary-based methods,[20] patch clamping techniques[21] and laminar stream delivery in microfluidic formats[22] have been shown to facilitate spatially specific membrane extraction. These approaches along with that of the SDM platform avoid destroying or solubilising entire cells and instead perform stepwise spatially selective sampling of the plasma membrane of single cells under controlled conditions using mechanical or chemical means. These methodologies are likely to overcome the problems pertaining to high abundance proteins masking low abundance proteins and thus will lower the need for complex downstream separation modules by performing upstream separation. The need to target the plasma membrane is a particularly pressing one as more traditional separation strategies based around *in-vivo* surface labelling followed by lysis and affinity capture[23] lead to only a 10–20% recovery rate for membrane proteins.[24–26]

1.2 Detergent based SDMs

Previous lipid based SDMs[11] were shown to act as triggers for membrane tether formation and reservoirs for the storage of extracted plasma membrane material during a process termed *nanodigestion*. Cell-SDM interactions are controlled using optical traps and monitored *via* a combination of brightfield and fluorescence imaging. Here we present a new type of SDM that does not rely on a physical approach linked to the excess membrane area stored in the plasma membrane. In this instance selective solubilisation of the plasma membrane is brought about by the controlled application of Triton X-100 coated SDMs that do not result in membrane tether generation. The experiments are conducted within a microfluidic device where a dual chamber format allows target cells to be physically stored in a separate compartment from the bulk SDM population. A laminar stream adjoining the two chambers prevents cross-contamination and unwanted cell-SDM interactions. The hydrophobic heptane core[27] provides the SDM with a refractive index that differs sufficiently from that of water to allow it to be manipulated using optical tweezers. Trapped Triton X-100 SDMs have been subsequently transferred from their bulk storage environment, across the laminar stream junction and into the cell storage chamber. At this point controlled cell-SDM interactions have been undertaken and the transfer of material between the cell and SDM has been observed.

2.0 Material and methods

2.1 Laser trapping and fluorescence imaging

Custom-built laser trapping optics (a combination of Linos Photonics, Qioptiq and Thorlabs Inc. parts) were fitted to the external port of a Nikon TE2000-E automated microscope, allowing optical manipulation with two laser beams (Fig. 1). For safe and compact containment of the laser beams and precluding the requirement of optics on the bench, the optical setup was attached to the modified supporting block (SB) of the microscope objective turret. The compact fibre coupled laser source used for trapping (IPG Photonics, YLM-5, 5W, 1070 nm, linear polarisation) was directly held in place by a set of modified cage plates (I1).

The manipulation of the two traps was facilitated by an optical arrangement consisting of a polarising beamsplitter (B1), two quarter-wave plates (λ/4) and two steering mirrors

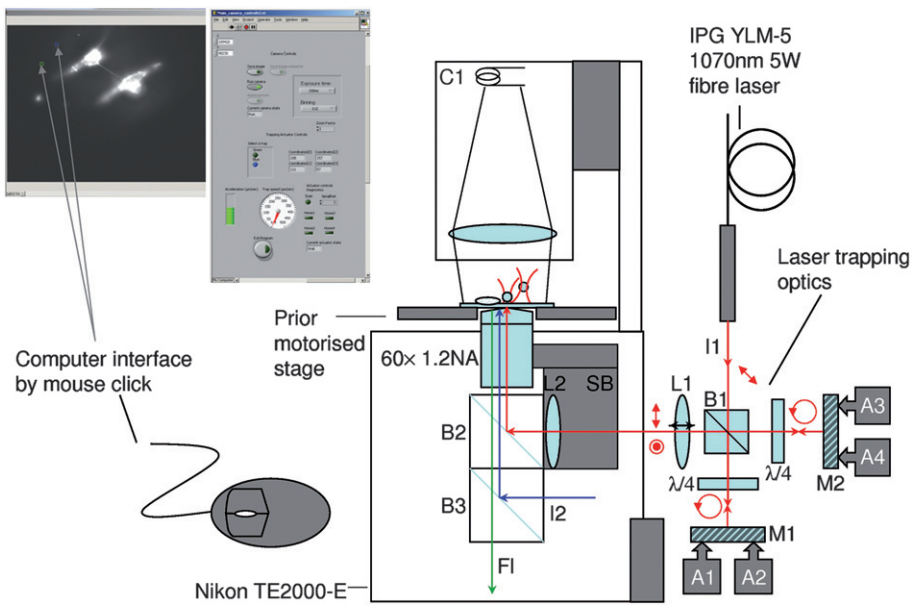

Fig. 1 Diagram of microscope used in trapping experiments with traps controlled by a custom written LabView mouse click interface. I1 = laser source input, B1 = polarising beamsplitter, M1-2 = 1064 nm infrared dielectric mirrors, λ/4 = quarter-wave plates, A1-4 = actuators, SB = supporting block of microscope turret, B2 = trapping dichroic for infrared, B3 = fluorescence (FITC) dichroic, I2 = fluorescence excitation input, Fl = light output to camera/eyepiece and C1 = trans-illumination, L1 = planovex anti-reflection coated lens (focal length = 100 mm), L2 = planovex anti-reflection coated lens (focal length = 100 mm).

(M1 and M2). To split the beam into two beams of equal intensity, the polarisation of the input laser was tilted at an angle of 45 degrees with respect to the s and p polarisation axes of the beamsplitter. This allowed the s and p polarisation components of the input beam to be split by the polarising beamsplitter and rotated by 90 degrees after double passing through the quarter-wave plates. This resulted in two beams of p and s polarisation, which were transmitted and reflected by the polarising beamsplitter respectively and steered by M1 and M2 independently.

Precise x–y steering of the optical tweezers was achieved by in-house modifications to the plane mirror mounts placed at each arm of the optical setup. Linear actuators (A1-4) (NSA-12, Newport, 11 mm range, 0.1 μm resolution), were fitted to these mirror mounts and connected up to an 8-axis switch box with hand held controller (NSC-SB and NSC-200 respectively, Newport). This was computer interfaced *via* a RS-485 to RS-232 converter (NSC-485-232-I, Newport) as part of the NewStep Expandable Motion Controller System (Newport). M1 and M2 were then imaged using a 1 × telescope (L1 and L2) onto the pupil plane of the microscope objective (60 × 1.2NA, water immersion, Nikon) to minimise the loss of power of the trapping beams when steering the traps in the image plane. Beam expansion of the original fibre laser output was unnecessary in this case as its output diameter (8 mm) was sufficiently large to fill the objective pupil. Fine repositioning of L1 was sufficient to refocus the traps in the focal plane of the objective and hence the position of any trapped object along the optical axis.

Modification to the SB of the microscope objective turret allowed accurate positioning of the trapping dichroic (B2) (Z900DCSP, Chroma) below the microscope objective. Underneath B2 was situated a filter cube carousel incorporating a FITC cube (B3) used for mercury lamp excitation (I2) and epifluorescence imaging (Fl) of EGFP labelled cells.

A cooled digital CCD camera (ORCA- ER, Hamamatsu) was situated on the left side port (100% transmission side) of the microscope for acquiring both bright field (*via* trans-illumination system (C1)) and fluorescence (*via* mercury lamp excitation) images. A motorised x-y stage was also utilised (Proscan, Prior) for fast screening of cells and manoeuvring of the stage and any microfluidic device over large distances relative to the microscope field of view and any SDMs trapped therein.

Traps were positioned by a mouse click in the field of view of a 512 × 512 pixel image, where the location of the trap was indicated by an overlaid coloured square. This interface written in LabView (LabView 8.1, National Instruments) controlled actuators A1-4 and was such that each trap moved sequentially along the x-axis of the image followed by movement along the y-axis. Additionally speed and acceleration of the traps could be varied by dials and sliders on the program's front panel. The Labview program also facilitated camera control including exposure time, binning and digital zoom and saving images in either 8 bit or 16 bit .png format.

2.2 Microfluidic chip layout and experimental protocol

To prevent unwanted cell-detergent interactions a microfluidic device was integrated with the trapping microscope set-up to facilitate isolation of the cell culture from the Triton X-100

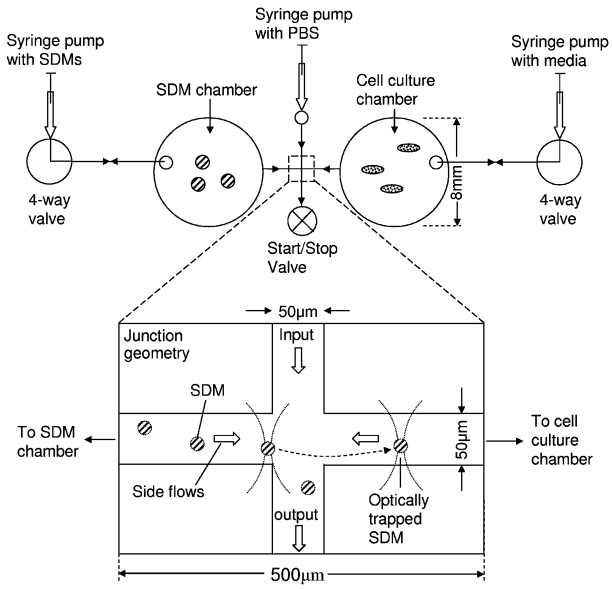

Fig. 2 Schematic of the microfluidic device operation for selectively trapping Triton X-100 coated SDMs and transferring them to the cell culture chamber for cell-SDM interactions. The junction acted as a valve isolating SDMs from the cell culture, preventing unwanted solubilisation of cells by the detergent. Flow direction is indicated by an arrow.

(Sigma-Aldrich) coated SDMs. A schematic of the polydimethylsiloxane (PDMS) (Sylgard 184 Elastomer Kit, VWR) microfluidic chip is shown in Fig. 2 illustrating the two main chambers, one for cell culture and one for SDM storage. The two chambers were linked to one another *via* a 50 μm wide channel, forming a junction with a second input/output 50 μm wide channel running perpendicular to it (all chambers and channels were 100 μm in depth). The cell culture and SDM chambers were connected up *via* PEEK tubing (10/32 finger tight fittings, Anachem Ltd) and external 4-way valves (Omnifit) to a 1 ml sterile disposable syringe with a Luer-lock fitting (Anachem Ltd) filled with cell culture media (high glucose DMEM, GibCo) and a glass 1 ml syringe filled with SDMs respectively. Both syringes were attached to separate syringe pumps (KDS200, KD Scientific). One of these syringe pumps (KDS200, KD Scientific) allowed for the pumping of two syringes simultaneously and was fitted with syringes for the input channel of the junction as well as the cell culture chamber (see Fig. 2). The function of the 4-way valves was to allow air bubbles to escape from the device and in particular from the central junction by pumping in PBS buffer at a flow rate of 5–10 μl/min from a 1 ml sterile disposable syringe down the input channel. To prevent the buffer flowing directly out of the chip, a start/stop valve was fitted to the output channel of the device *via* PEEK tubing (see Fig. 2).

Once air bubbles were removed from the chip, the start/stop valve was opened and the volumetric flow rate of the PBS and media streams reduced to 200 nl/min. SDMs were then injected into the device at an initially higher flow rate of 5–10 μl/min, which was then reduced upon SDMs reaching the junction to 30 ± 0.3 nl/min to balance the opposing flow rate from the cell culture chamber.

The LabView program was then initiated and a manual search using the motorised stage used to locate and trap optically

appropriate SDMs (sized between 1–4 μm). Once an SDM was trapped (using typical laser powers of 100 mW at the pupil plane of the objective, typically 40–60% transmission to the sample plane at 1070 nm[28]) the motorised stage was used again to locate a suitably polarised and EGFP expressing cell in the culture chamber.

SDMs were then moved across the junction to the cell chamber containing cultured human BE colon carcinoma cells with CAAX EGFP labelled motif (see section 2.5) to perform cell-SDM experiments using optical tweezers. Unwanted flooding of the cell culture chamber with SDMs, detergent monomers or vesicles was prevented by the junction acting as a valve and directing all flows towards the output channel.

SDMs were manoeuvred and then contacted to the plasma membrane of target cells for time periods in excess of 30 seconds. It was found that shorter incubation times were not sufficient to promote material transfer. After between 60 and 300 seconds of contact the SDM was moved away from the cell at a rate of 5–10 μm/sec.

2.3 Microfluidic device fabrication

Microfluidic channels of rectangular cross section (typically width × height = 50 × 100 μm) were produced from master templates. These were made from UV cured 100 μm thick SU-8 100 photoresist (MicroChem) spin coated at 3000 rpm for 30 secs onto 100 mm diameter, 525 ± 25 μm thick Silicon wafers (IDB Technologies Ltd). Negative photomasks were designed in AutoCad 2008, printed onto thin acetate sheets and placed on the SU-8 coated wafers prior to exposure.

Moulded PDMS substrates were fabricated by mixing an elastomer precursor with a resin-based cross-linking agent (Sylgard 184 Elastomer Kit, VWR) at a ratio of 10:1 and pouring it onto the master template. The PDMS was then left to cure overnight, or for more rapid curing, left on a hot plate at 65 °C for 3 hours. Air bubbles trapped in the cured PDMS structure were prevented by pre-treatment of the PDMS under vacuum. Removal of the final PDMS structure from the master was achieved by use of a sharp scalpel blade, after which the PDMS was sliced into 24 × 50 mm coverglass sized rectangular chips. A schematic of the microfluidic device containing 100 μm deep channels is shown in Fig. 3.

To enable fluid delivery from external tubing, holes were punched through the PDMS substrate using a belt puncture. Fluid inlet and outlet fittings were made by attaching PEEK tubing (internal diameter 254 μm, external diameter 1.8 mm, Anachem Ltd) to 2 mm holes in 24 × 50 mm microscope slides (1.0–1.2 mm standard thickness microscope slides, VWR) and glued with Araldite. Holes in the glass were made slowly and carefully using a mini high speed drill fitted with a 2 mm diamond burr drill head (Diama ltd) and using copious amounts of water as coolant.

These microscope slides formed the top layer of the entire microfluidic device.

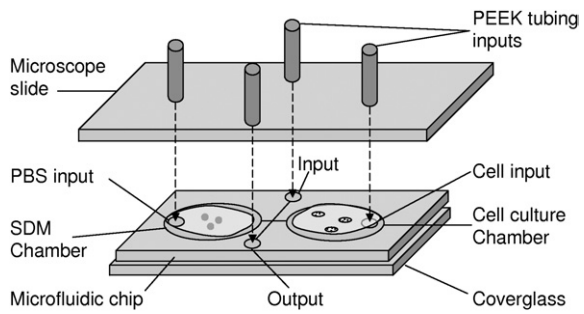

Fig. 3 Schematic of the microfluidic chip used to facilitate cell-SDM interactions.

2.4 Chip assembly and cell loading

Prior to chip assembly all coverglass and microfluidic substrates were cleaned with ethanol in a disposable sterile plastic culture dish, dried using nitrogen free oxygen and left in a culture hood for 3 hrs to ensure complete removal of ethanol. This was essential to sterilise the chambers, clean the surfaces for more effective bonding to microscope slide and coverglass and to prevent small dust particles from blocking the microfluidic channels. Coverglass slides formed the bottom surface of the microfluidic device and to reduce any possible spore or bacterial growth, UV 2sterilisation was performed in the culture hood overnight.

The PDMS substrate was then mounted between a coverglass and microscope slide with the channel and chamber facing the coverglass surface. Care was taken to push out any remaining air bubbles to ensure good bond between the PDMS and glass surfaces. This method of producing a firm but non-permanent bond between the chip and coverglass was found to be sufficient and also convenient under the applied experimental conditions *i.e.* low operational fluid pressures (<10 μl/min). This also precluded the additional step of using a plasma oven, which facilitates permanent bonding between the PDMS and glass surfaces.

After cell splitting, and to reduce clumping, cells were resuspended in growth media by pipetting up and down for 30 seconds. This suspension was then transferred into a sterile 30 ml Sterilin tube (see cell culture protocols, Section 2.5). Cells were then loaded into the assembled chip *via* the access holes of the cell culture chamber by gently inserting a Gilson pipette into the cell input and manually pipetting in 20 μl (Gilson 20 μl filtered pipette tips) of the cellular suspension. To prevent evaporation of media into the second chamber, this was filled with 20 μl of sterile PBS buffer (pH 7.4). Chips loaded with cells were placed into sterile disposable culture dishes and stored in the cell culture incubator at 37 °C for cell attachment and polarisation.

2.5 Cell culture protocols

Adherent human colon carcinoma cells (BE cells) were fluorescently labelled with EGFP-Tk (EGFP labelled CAAX motif of K-Ras) at the plasma membrane[29] (a kind gift from Dr Hugh Paterson at The Institute of Cancer Research, London). Cells were cultured at 37 °C and 5% CO_2 in 25 cm^2 filter capped flasks containing phenol free media (high glucose DMEM, GibCo) with 10% Foetal Calf Serum, 100 μl/ml Penicillin and 100 μg/ml Streptomycin. Upon reaching 80% confluency, cells were split in a culture hood by removal of culture media, washing with sterile phosphate buffered saline (PBS) (pH7.4, GibCo) and incubation with 2 ml of trypsin solution (Sigma-Aldrich) containing trypsin 5 g/ml and EDTA 2 g/ml diluted to 10% in PBS for 2–3 minutes.

Following cell detachment, 5 ml of culture media was added to the flask and the cells were gently re-suspended by pipetting up and down for 30 seconds before adding to microfluidic chips.

2.6 Triton X-100 SDM emulsion stock production

To produce a relatively stable SDM emulsion stock lasting for several months, 1 ml of Triton X-100 (1.7M) was added to 2.8 ml of distilled water in a 30ml screw capped glass vial. The solution was then warmed on a hot plate at 50 °C and gently stirred occasionally until the Triton X-100 had fully dissolved. 7.8 ml of Heptane (99.0% purity) was then pipetted into the vial containing the detergent solution. To emulsify the mixture fully the stock solution was shaken vigorously and vortexed for about 1 minute. For use in microfluidic experiments the stock was diluted 1:10 in PBS and 1ml of this was used to fill a glass syringe to pump SDMs into one of the microfluidic chambers.

2.7 Dynamic light scattering measurements (DLS)

A HPPS unit (Malven Instruments) was used to determine the size distribution of the SDMs. 20 μl of the SDM emulsion (Section 2.6) was diluted in 5 ml of water and the resulting solution transferred into a sample cell until the sample cell was topped up to ~1.5 cm.

3.0 Results and discussion

Within full cell lysis strategies, solubilisation of membrane fractions including those of plasma membranes is typically initiated by the application of surfactants such as sodium dodecyl sulfate (SDS), Triton X-100, CHAPS, octylglucoside and Zwittergent 3–12. Detergent to protein ratios are often individually optimized as this ratio is crucial to the solubilisation of a given protein type. However, despite being able to refine the protein-detergent ratios the flexibility of these detergent systems is hampered by the fact that they are presented to populations of cells using bulk micellar preparations of surfactants with little or no spatial or temporal control of cell–detergent interactions. Instead, complex downstream separations are undertaken to overcome these issues.

During these experiments we aimed to use a new approach in which SDMs consisting of Triton X-100 coated heptane droplets were brought into contact with cells expressing membrane localised EGFP. The SDM-cell interactions were controlled using optical traps and separate chambers for the cell growth and SDM storage.

DLS measurements were used to determine the size of the SDMs. It was possible to generate a number of stable SDM distributions ranging in size from less than 1 μm to tens of microns. Although the smaller sized SDMs could be used for nano-scale sampling of the cell membrane they were difficult to observe under bright field microscopy and hence non-trivial to trap optically. Larger sized SDMs (1–4 μm) were straightforward to trap optically and thus selected for our cell-SDM interaction experiments. Furthermore, trapped n-heptane emulsion droplets were found to be stable for time periods greater than 20 minutes, unlike emulsion droplets made from other alkanes *e.g.* hexane, which were found to be stable for less than 3 minutes when held in the optical trap.

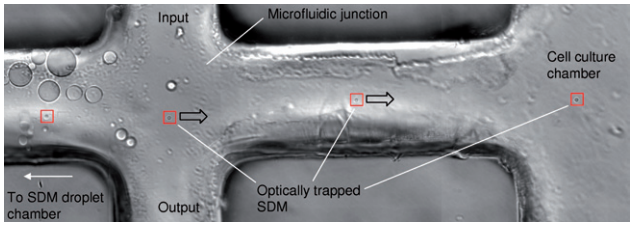

Fig. 4 Image montage of a microfluidic device for nanodigestion. The square shows a trapped SDM with the arrows indicating the direction of trap movement by stage scanning (channel width = 50 μm).

Using the protocols described in Section 2.0, BE human carcinoma cell–Triton X-100 SDM interactions were monitored using a combination of brightfield and fluorescence microscopy. Fig. 4 depicts the transfer of a Triton X-100 SDM (~3 μm in size) from the storage chamber (LHS) to the cell culture chamber (RHS).

Experiments were conducted on both trypsinised and untrypsinised BE human carcinoma cells expressing membrane localized EGFP. In the former case cells were used immediately after introduction into the microfluidic device and not allowed to attach themselves fully to the coverglass. Following an incubation time of 30 seconds between a target cell and a Triton X-100 based SDM, membrane tether formation was not observed (Fig. 5). This is in contrast to SDMs[11] composed of a hexadecane hydrocarbon core and fusogenic lipid outer coating (1,2-dioleoyl-phosphatidylethanolamine and 1,2-dioleoyl-sn-glycero-3-phosphatidylcholine) which have been shown to drive membrane tether formation under similar conditions. Variations in both the

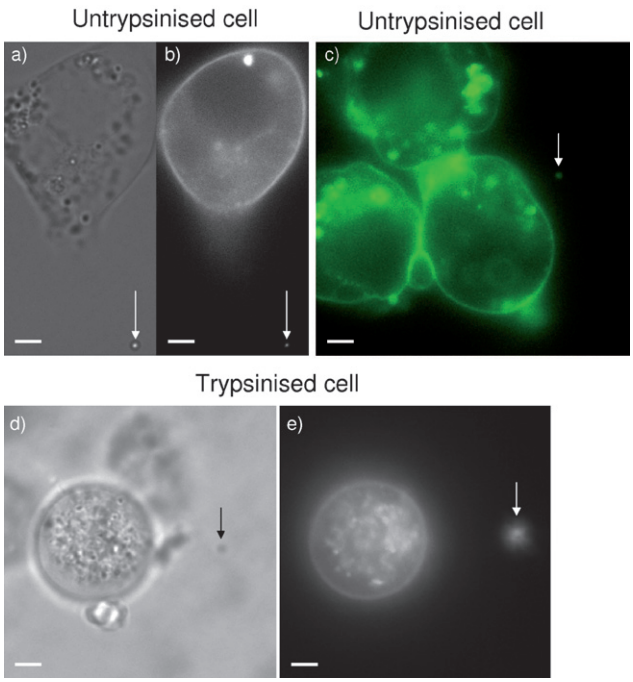

Fig. 5 Images of SDM- trypsinised and untrypsinised cell interactions after 60 seconds (a–c) and (d–e) 300 secs. (a) and (d) show brightfield images of BE cells prior to SDM contact and (b), (c) and (e) show fluorescent images illustrating the transfer of membrane localised EGFP to the SDM. Scale bar = 4 μm.

incubation time, laser power (up to 150 mW) and rate (up to 0.5 μm/sec) at which the SDMs were pulled from the target cell failed to promote tether formation.

A key observation in this previous study was the uptake of membrane localised EGFP from the inner leaflet of the plasma membrane of the cell to not only the membrane tether but also to the surface of the SDM itself. In effect the tether acts as a vehicle for material transfer. As can be seen from Fig. 5, transfer of EGFP localized to the inner leaflet of the plasma membrane is again observed despite the absence of tether formation.

Preliminary results indicate an approximate success rate of 70% observed for EGFP material transfer from trypsinised cells. These initially provided a simpler system for study as the protein machinery on the cell surface responsible for cell adhesion had been digested during the trypsinisation process. This minimizes physical barriers to SDM–cell interactions. When corresponding experiments were conducted with untrypsinised cells (Fig. 5) similar success rates were observed (~70%). This is a crucial observation as the viability of using Triton X-100 based SDMs as a proteomic tool for spatially sampling the plasma membrane of a given cell will be maximised by minimizing any chemical and or/biological modifications to the cells prior to sampling. In the absence of membrane tether formation the uptake of EGFP to the SDM is believed to be the result of localized membrane solubilisation effected by the action of the Triton X-100 on the surface of the SDM. As can be seen from Fig. 5 the use of an SDM as a delivery vehicle for the Triton X-100 to the cell surface allows us to locally probe with spatially specificity the plasma membrane of a target cell without performing full cell lysis. Furthermore, when the SDM is withdrawn from the area of interest it remains stable in the optical trap allowing it to be transferred from the cell culture chamber and moved downstream to analysis modules with retention of the SDM cargo.

4.0 Conclusions

We have demonstrated a new technique capable of effecting spatially selective chemical digestion of single cells in a controlled microfluidic environment. By separating the SDM storage chamber and the cell culture environment using a laminar stream and manipulating interactions using optical traps we are able to control both the spatial and temporal aspects of SDM–cell interactions.

Future work will include developing methodologies capable of identifying which proteins have been excised by application of the SDM. This will open up the exciting possibility of being able to conduct spatially resolved proteomic analysis of single cells. Experiments toward this goal are currently underway in our laboratories.

Acknowledgements

We thank the EPSRC for the award of grant EP/C54269X/1 and Platform grants GR/S77721 and EP/C541839/1. We would like to thank Dr Haley Cordingley for helping to establish the microfluidic platforms used during these experiments.

References

1 J. E. Ferrell and E. M. Machleder, *Science*, 1998, **280**, 895–898.
2 T. Y. Huang, T. F. Chu, H. I. Chen and C. Y. J. Jen, *Faseb Journal*, 2000, **14**, 797–804.
3 M. N. Teruel and T. Meyer, *Science*, 2002, **295**, 1910–1912.
4 J. S. Marcus, W. F. Anderson and S. R. Quake, *Analytical Chemistry*, 2006, **78**, 956–958.
5 D. Di Carlo, K. H. Jeong and L. P. Lee, *Lab Chip*, 2003, **3**, 287–291.
6 C. V. Rao, D. M. Wolf and A. P. Arkin, *Nature*, 2002, **420**, 231–237.
7 G. T. Roman, Y. L. Chen, P. Viberg, A. H. Culbertson and C. T. Culbertson, *Analytical and Bioanalytical Chemistry*, 2007, **387**, 9–12.
8 C. E. Sims and N. L. Allbritton, *Lab Chip*, 2007, **7**, 423–440.
9 B. Huang, H. K. Wu, D. Bhaya, A. Grossman, S. Granier, B. K. Kobilka and R. N. Zare, *Science*, 2007, **315**, 81–84.
10 H. Zhang and W. R. Jin, *Journal of Chromatography A*, 2006, **1104**, 346–351.
11 P. M. P. Lanigan, K. Chan, T. Ninkovic, R. H. Templer, P. M. W. French, A. J. de Mello, K. R. Willison, P. J. Parker, M. A. A. Neil, O. Ces and D. R. Klug, *Journal of The Royal Society Interface*, 2008, **5**, S161–S168.
12 P. A. Quinto-Su, H. H. Lai, H. H. Yoon, C. E. Sims, N. L. Allbritton and V. Venugopalan, *Lab Chip*, 2008, **8**, 408–414.
13 E. A. Schilling, A. E. Kamholz and P. Yager, *Analytical Chemistry*, 2002, **74**, 1798–1804.
14 K. R. Rau, P. A. Quinto-Su, A. N. Hellman and V. Venugopalan, *Biophysical Journal*, 2006, **91**, 317–329.
15 H.-H. Lai, P. A. Quinto-Su, C. E. Sims, M. Bachman, G. P. Li, V. Venugopalan and N. L. Allbritton, *Journal of The Royal Society Interface*, 2008, **5**, S113–S121.
16 J. Zimmerberg and M. M. Kozlov, *Nat. Rev. Mol. Cell Biol.*, 2006, **7**, 9–19.
17 G. Ocvirk, H. Salimi-Moosavi, R. J. Szarka, E. A. Arriaga, P. E. Andersson, R. Smith, N. J. Dovichi and D. J. Harrison, *Proceedings of the Ieee*, 2004, **92**, 115–125.
18 H. Sedgwick, F. Caron, P. B. Monaghan, W. Kolch and J. M. Cooper, *Journal of The Royal Society Interface*, 2008, **5**, S123–S130.
19 J. Dragavon, T. Molter, C. Young, T. Strovas, S. McQuaide, M. Holl, M. Zhang, B. Cookson, A. Jen, M. Lidstrom, D. Meldrum and L. Burgess, *Journal of The Royal Society Interface*, 2008, **5**, S151–S159.
20 J. A. Jonsson and L. Mathiasson, *Chromatographia*, 2000, **52**, S8–S11.
21 B. Sakmann and E. Neher, *Annual Review of Physiology*, 1984, **46**, 455–472.
22 S. Takayama, E. Ostuni, P. LeDuc, K. Naruse, D. E. Ingber and G. M. Whitesides, *Chemistry & Biology*, 2003, **10**, 123–130.
23 M. J. Peirce, R. Wait, S. Begum, J. Saklatvala and A. P. Cope, *Molecular & Cellular Proteomics*, 2004, **3**, 56–65.
24 J. Blonder, M. B. Goshe, R. J. Moore, L. Pasa-Tolic, C. D. Masselon, M. S. Lipton and R. D. Smith, *Journal of Proteome Research*, 2002, **1**, 351–360.
25 D. K. Han, J. Eng, H. L. Zhou and R. Aebersold, *Nature Biotechnology*, 2001, **19**, 946–951.
26 M. P. Washburn, D. Wolters and J. R. Yates, *Nature Biotechnology*, 2001, **19**, 242–247.
27 M. G. B. Andrew, D. Ward, Christopher D. Mellor and Colin D. Bain, *Chem. Commun.*, 2006, 4515–4517.
28 K. C. Neuman, E. H. Chadd, G. F. Liou, K. Bergman and S. M. Block, *Biophys. J.*, 1999, **77**, 2856–2863.
29 A. Apolloni, I. A. Prior, M. Lindsay, R. G. Parton and J. F. Hancock, *Mol Cell Biol*, 2000, **20**, 2475–2487.